SRTTU

JCARME
ISSN: 2228-7922
Journal of Computational and Applied Research in Mechanical Engineering
Vol. 9, No. 2, pp. 235-243
jcarme.sru.ac.ir

High-velocity impact properties of multi-walled carbon nanotubes/E-glass fiber/epoxy anisogrid composite panels

Hamed Khosravi[a, b] and Reza Eslami-Farsani[a,*]

[a] *Faculty of Materials Science and Engineering, K. N. Toosi University of Technology, Tehran, Iran.*
[b] *Department of Materials Engineering, Faculty of Engineering, University of Sistan and Baluchestan, Zahedan, Iran.*

Article info:

Received:	20/05/2018
Revised:	06/11/2018
Accepted:	08/11/2018
Online:	10/11/2018

Keywords:
Grid panels, Multi-walled carbon nanotubes, Silanization, Ballistic limit, Energy absorption.

Abstract
This work reports the high-velocity impact response of multiscale anisogrid composite (AGC) panels. The aim of the present study is to evaluate the influence of surface-modified multi-walled carbon nanotubes (S-MWCNTs) at different S-MWCNTs contents (0-0.5 wt.% at an interval of 0.1 wt.%) on the high-velocity impact responses of E-glass/epoxy AGC. Surface modification of MWCNTs is confirmed by Fourier-transform infrared (FTIR) and thermogravimetric (TGA) analyses. AGC panels were fabricated via a manual filament winding technique. E-glass fiber roving and E-glass woven fabric are employed as reinforcing agents in ribs and skin, respectively. The impact test is done on the composite panels by a cylindrical projectile with a conical nose. The results showe that the highest enhancement in the impact characteristics is attributed to the panel containing 0.4 wt.% S-MWCNTs. Based on the analysis of fracture surfaces, enhanced interfacial fiber/matrix bonding is observed for the S-MWCNTs loaded specimen. Furthermore, the incorporation of MWCNTs leads to the reduced damaged area and enhanced tolerance of damage.

1. Introduction

Using grid-stiffened composites (GSCs), as advanced and high-performance structures, is increasing in aerospace, aircraft, and automotive industries. GSC structures are considered as preferred substitutes for common components [1, 2]. They are thin shell structures having helical or axial ribs in their network, where the ribs bear the most of the applied load [3, 4]. Several research works have been done on the design and preparation of these structures [1-8].
The composite materials are very susceptible to damages caused by various types of loadings, and their behavior in the presence of damages should be properly understood. Energy absorption capability which can be defined as the resistance of impact-exposed composite to penetration and perforation is a critical factor for high technology applications [9]. There exist various mechanisms for energy absorption of fibrous composites such as matrix cracking, shear plugging, and delamination [10].
Due to extensive applications of fiber-reinforced polymers (FRPs), several works have been reported on the mechanical properties of these

[*] *Corresponding author*
email address: eslami@kntu.ac.ir

structures [11-13]. The matrix modification of FRPs through the incorporation of nanoparticles can further increase their mechanical properties [14-16]. Among the various types of nanofillers, the very favorable mechanical properties of CNTs and their high aspect ratio make them ideal reinforcing material for polymer composites [17]. Literature review on the various properties of CNTs indicates the high elastic modulus and strength of this type of materials [18]. According to the literature, several works have been performed on the mechanical behaviors of CNT-loaded nanocomposites [19-23]. For example, Pandya et al. [20] found that through the incorporation of 0.5 wt.% CNTs, the energy absorption capability of the epoxy/glass fiber specimen enhanced by 25%. Rahman et al. [21] showed that the ballistic-limit of the epoxy/glass fiber specimen increases through the incorporation of 0.3 wt.% MWCNTs. Laurenzi et al. [22] investigated the impact resistance behavior in CNTs filled epoxy. They found that the CNT-reinforced panels demonstrate an enhanced ballistic response in comparison with the neat ones. Rahman et al. [23] found that the flexural strength and modulus of the epoxy/glass fiber specimen increase by 38% and 22%, respectively, with the introduction of 0.3 wt.% CNTs.

A scan through the literature illustrates little research works have been done on using nanoparticles as reinforcement in GSC structures [24-26]. Herein, the impact response of MWCNTs filled GSC panels is assessed. The energy absorption capability and ballistic-limit velocity of the specimens are reported and compared.

2. Experimental

2.1. Materials

The matrix resin used in composites for the current study is ML-506 epoxy resin based on epoxy bisphenol F with hardener HA-11, supplied by Mokarrar Engineering Materials Co, Iran. The resin- hardener ratio is 100:15 by weight, as recommended by the manufacturer. This resin system is chosen because of its low viscosity (1450 centipoise) and long gel time (60 min) at 25 °C. Also, the mixed system density is 1.1 g/cm^3. The tensile and flexural strengths of employed resin are 761 and 960 kgF/cm^2, respectively. Unidirectional E-glass fiber (density: 2.58 g/cm^3, average diameter: 12 μm) and 2-dimensional plain weave E-glass fabric (surface density: 400 g/m^2), both supplied by LINTEX International Co., Ltd, China, are used as fibrous reinforcements. The silica nanoparticle, as filler part, are purchased from US Research Nanomaterials, Inc, USA. Fig. 1 illustrates an FE-SEM image of as-received silica nanoparticles. These particles have an average particle size of 65 nm and a specific surface area of 380 m^2/g.

3-glycidoxypropyltrimethoxysilane (3-GPTS), as a silane coupling agent, is provided by Merck Chemical Co, Germany. The molecular formula of the 3-GPTS is $C_9H_{20}O_5Si$. This compound is selected because of its epoxide groups which can easily react with epoxy matrix in the presence of amine hardener.

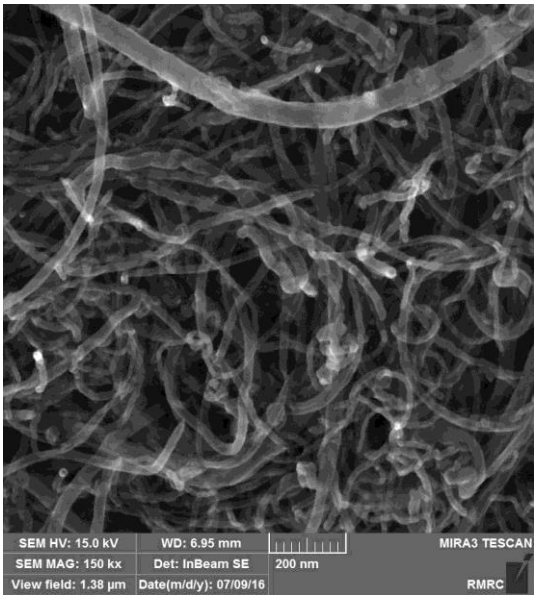

Fig. 1. SEM image of as-received MWCNTs.

2.2. Surface modification of MWCNTs

In the first step, 0.5 g MWCNTs (Table 1) is added to the 100 mL solution (95 mL ethanol-5 mL water). After that, 3-GPTMS coupling agent (silane/CNT weight ratio: 1/1) is incorporated into the solution. In the next step, the mixture is sonicated for 10 min and refluxed for 8 h at a temperature of 80°C. The pH of the solution is

regulated at around 4.5 by HCl (37%) acid [27]. To separate the silanized MWCNTs (S-MWCNTs), the resultant mixture is centrifuged for 8 h. In the final step, obtained powders are washed twice with ethanol and then dried in an oven.

Table 1. Details of MWCNTs.

Diameter (nm)	Length (μm)	COOH content (gr/cm^3)	Specific area (m^2/g)
10-20	20-30	2	233

2.3. Preparation of GSC panels

Various weight percentages of S-MWCNTs (0-0.5 wt.% at an interval of 0.1) are added to the epoxy resin. After initial mechanical stirring by an overhead mechanical stirrer, ultrasonic waves are applied to the mixture for 90 min [24]. After mixture degassing, the curing agent is added drop-to-drop. The panels are fabricated via a manual filament winding route. At the initial stage, pre-impregnated unidirectional E-glass fibers are placed into the silicone mold grooves (Fig. 2) to establish the ribs. Then, the skin is laid up using four layers of E-glass fabrics over the network of ribs. Fabricated specimens are shown in Fig. 3. The panels are cured at room temperature. The characteristics of specimens are displayed in Table 2.

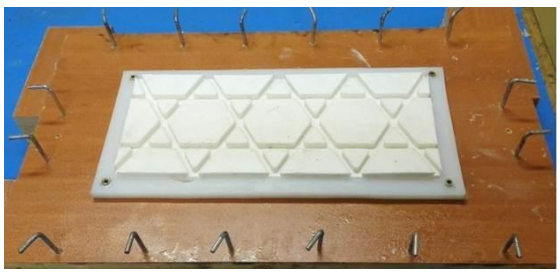

Fig. 2. The fabricated silicone mold.

2.4. Impact test

For conducting the impact test, an aluminum cylindrical projectile with a conical nose, as indicated in Fig. 4, is used. The weight of the projectile is 27 g. The position of the specimens when exposed to the impact loading can be seen in Fig. 5. The GSC specimens with a dimension of 15 × 15 cm^2 are used.

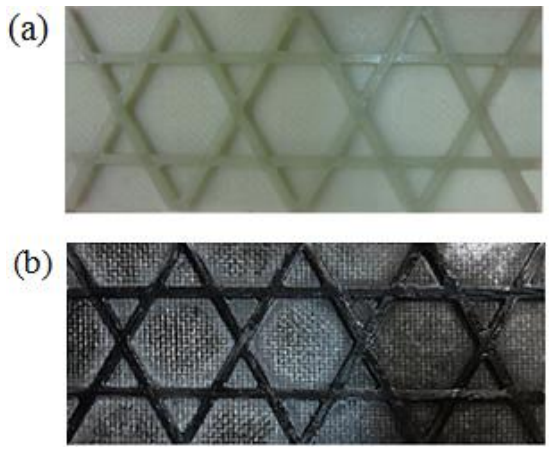

Fig. 3. Fabricated specimens; (a) neat and (b) multiscale.

Table 2. Characteristics of the fabricated specimens

Rib cross section (mm^2)	Length (mm)	Width (mm)	Skin thickness (mm)
6×6	300	125	1.8

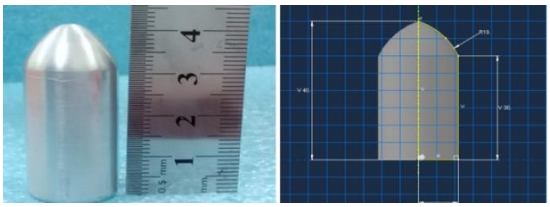

Fig. 4. Conical cylindrical projectile.

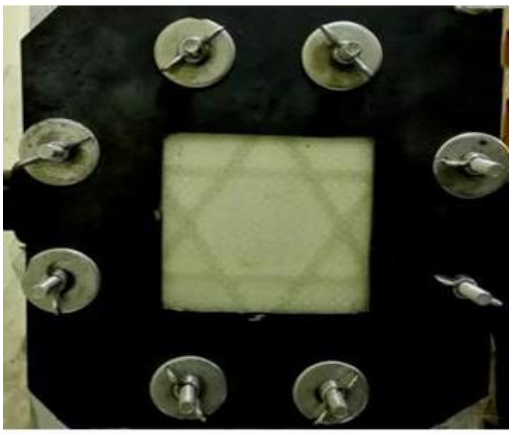

Fig. 5. GSC specimen in the fixture of the impact test.

The impact response of the specimens is reported in terms of impact-limit velocity (V_{50}) and the amount of energy absorption (E_{abs}), calculated from the following equations [28]:

$$V_{50} = \sqrt{V_i^2 - V_r^2} \quad (1)$$

$$E_{abs} = \frac{1}{2} m_p (V_i - V_r)^2 \quad (2)$$

2.5. Characterization

To characterize the silanized MWCNTs, Fourier-transform infrared (FTIR) spectrometer (JASCO, 460-plus) in the 400-4000 cm^{-1} range (resolution: 4 cm^{-1}) is employed. TGA analysis (model: STA504) is conducted in a nitrogen atmosphere (temperature range: 25-800°C, and heating rate: 10°C min^{-1}). The fracture surface of specimens after impact test is examined using a field emission electron microscopy (FESEM- MIRA3 TESCAN).

3. Results and discussion

3.1. Results of FT-IR and TGA

The surface properties of COOH-MWCNTs and S-MWCNTs are studied using FTIR analysis. FTIR spectra of these powders are displayed in Fig. 6. Regarding the FTIR spectrum of COOH-MWCNTs, the observed bands at 1716.5 cm^{-1} and 1156.6 cm^{-1} show the C-O and C=O stretching vibrations, respectively [29]. The bands at 2519.7 cm^{-1} and 3179.5 cm^{-1} show the presence of OH groups, and the peaks at 801.5 cm^{-1} and 1412.9 cm^{-1} indicate the bending deformation of OH [30]. The appearance of two bands at 1592.7 cm^{-1} and 2872.9 cm^{-1} is related to the presence of C-H and C=C. On the contrary, an extra peak is visible in the FTIR spectrum of modified CNTs at 852 cm^{-1}, indicating the formation of Si-O-C [31]. These results clearly show that the silane compound is grafted on the surface of CNTs. Fig. 7 shows the TGA weight loss data over a range of temperatures for COOH-MWCNTs and S-MWCNTs. As indicated in this figure, the weight loss for S-MWCNTs at 500°C is higher than that of COOH-MWCNTs, which is due to the 3-GPTMS thermal decomposition.

3.2. Impact response

The results of impact properties for different S-MWCNTs loadings are shown in Fig. 8. As indicated, the introduction of S-MWCNTs to the matrix of composites can affect the impact response of panels. A summary of the results of the impact test for various specimens is shown in Table 3. As it is observed from Fig. 8 and Table 3, through the incorporation of 0.4 wt.% S-MWCNTs, the values of ballistic limit velocity and energy absorption capability of the E-glass/epoxy GSC specimen increase by 11% and 23%, respectively, compared to the neat specimen.

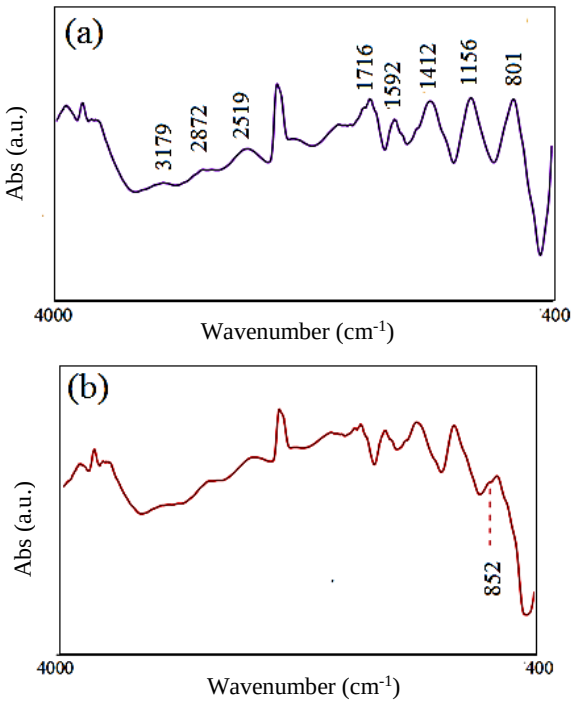

Fig. 6. FT-IR spectra of a) COOH-modified MWCNTs, and b) silane-modified MWCNTs.

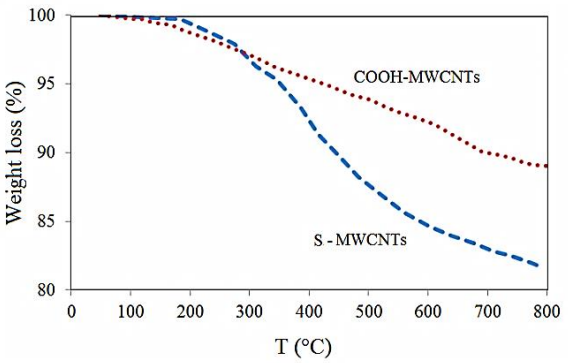

Fig. 7. TGA results of COOH-modified and silane-modified MWCNTs.

It seems that the observed increase in the impact responses of the multiscale specimens having S-MWCNTs is as a result of the following reasons: first, by reinforcing the matrix through the S-MWCNTs addition, the frictional slippage of the interface is hindered because of the presence of S-MWCNTs. This indicates that for specimens containing S-MWCNTs, an efficient transferring of the applied load between the matrix and fibers can be occurred [32-34]. Thus, the impact properties of the specimens, including S-MWCNTs, are higher than control specimen.

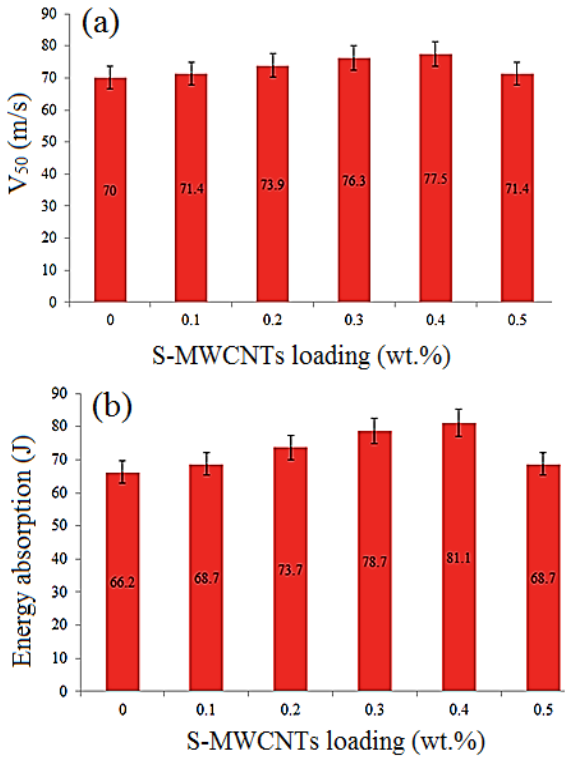

Fig. 8. The values of (a) V_{50} and (b) energy absorption of GSC panels reinforced with various contents of S-MWCNTs.

Table 3. The values of impact results.

S-MWCNTs (wt. %)	Initial velocity (m/s)	Residue velocity (m/s)	V_{50} (m/s)	Absorbed energy (J)
0	120	95	70	66.2
0.1	120	94	71.4	68.7
0.2	120	92	73.9	73.7
0.3	120	90	76.3	78.7
0.4	120	89	77.5	81.1
0.5	120	94	71.4	68.7

The second reason is related to this fact that modulus of S-MWCNTs is higher than epoxy matrix [35, 36]. Third, MWCNTs can act as rigid barriers against the crack initiation and propagation, via crack bridging [37]. So, a higher amount of energy for crack growth is required. Forth, the rib-skin adhesion can be enhanced due to the S-MWCNTs addition. This suggests that GSC specimens reinforced with S-MWCNTs have higher energy absorption than the neat specimen. The observed drop in the impact characteristics of the 0.5 wt.% S-MWCNT loaded specimen is related to the decrement of adhesion in the fiber-matrix interface due to the CNT agglomerate formation at higher S-MWCNT loading as a result of the increased viscosity of the resin. The presence of CNT agglomerates can create regions of stress concentration [38]. As can be seen in Fig. 9, with the addition of S-MWCNTs, the damage size decreases due to the higher bending stiffness of CNT loaded specimen.

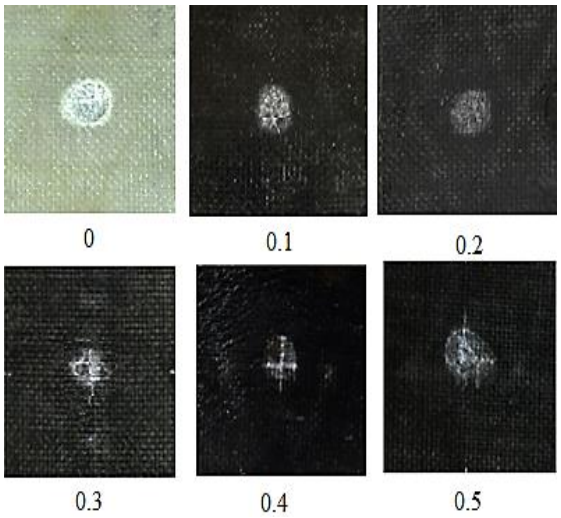

Fig. 9. Damaged area of GSC specimens containing various weight contents of S-MWCNTs.

In GSC composites, some of the main energy absorption mechanisms in the high-velocity impact test are delamination, matrix cracking, fiber breakage, and perforation. By the addition of CNTs, delamination resistance is enhanced as a result of improved matrix-fiber interface bonding. In fact, in MWCNTs loaded specimens less delamination is observable. Accordingly, the size of the damaged area is declined.

However, for the specimen reinforced with 0.5 wt.% CNTs compared to the 0.4 wt.% CNTs loaded one, the damaged area increases due to the improper dispersion of MWCNTs within the polymeric matrix. In fact, agglomeration of S-MWCNTs causes the reduction of delamination resistance of composite, and as a result, the damaged area increases.

3.3. Microstructural examination

The surface morphology of the unfilled and filled GSCs after impact test is investigated by FESEM. The fracture surface of the neat composite illustrates that the epoxy matrix is separated from the fibers due to the poor adhesion, as indicated by the clean surface of the fibers (Fig. 10a). Fig. 10b illustrates the presence of adhered matrix to the surface of glass fibers, showing a considerable bonding between the fibers and matrix for the nanocomposite specimen. From Fig. 10c, uniform dispersion of CNTs within the matrix is observable. Moreover, CNTs are seen on the fracture surface in the form of pulled out or broken, manifesting the existence of crack bridging [39].

4. Conclusions

In the present work, the behavior of AGS composites filled with various loadings of S-MWCNTs is investigated under high-velocity impact test. The main results obtained from this study are as follows:

1. Surface modification of MWCNTs is confirmed by FTIR and TGA analyses.
2. Ballistic limit and energy absorption of the AGS specimen containing 0.4 wt.% S-MWCNTs enhance by 11% and 23% over the neat specimen.
3. The introduction of S-MWCNTs enhances the interfacial bonding between the E-glass fiber and polymeric matrix.
4. The introduction of S-MWCNTs decreases the damage size of specimens exposed to the high-velocity impact.

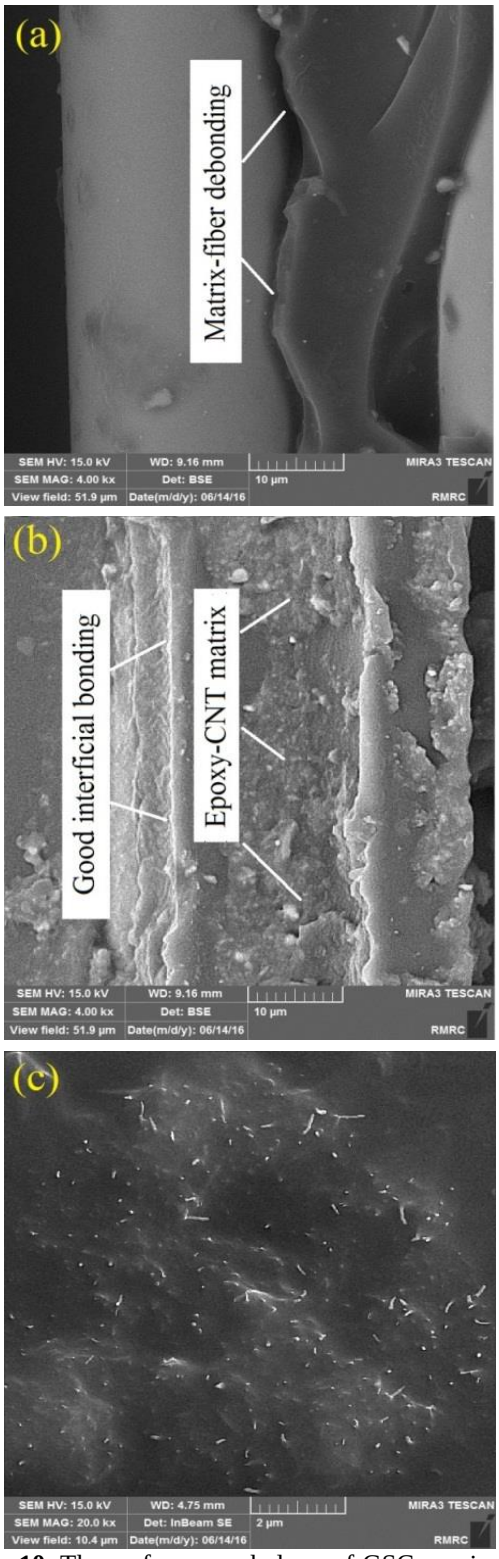

Fig. 10. The surface morphology of GSC specimens after impact test, a) non-filled specimen, b) containing 0.4 wt.% S-MWCNTs, and c) High magnification image from the matrix of 0.4 wt.% reinforced specimen.

References

[1] V. V. Vasiliev, and A. F. Razin, "Anisogrid composite lattice structures for spacecraft and aircraft applications", *Composite Structures*, Vol. 76, No. 1-2, pp. 182-189, (2006).

[2] V. V. Vasiliev, V. A. Barynin, A.F. Rasin, S.A. Petrokovskii, and V.I. Khalimanovich, "Anisogrid composite lattice structures-development and space applications", *Composite structures*, Vol. 94, No. 3, pp. 38-50, (2009).

[3] J. Eskandari-Jam, M. Noorabadi, H. Taghavian, M. Mohammadi, and N. Namdaran, "Design of anisogrid composite lattice conical shell structures", *Journal of Science and today's world*, Vol. 7, No. 9, pp. 140-146, (2013).

[4] C. Gan, R. F. Gibson, and G. Newaz, "Analytical/experimental investigation of energy absorption in grid-stiffened composite structures under transverse loading", *Experimental Mechanics*, Vol. 44, No. 2, pp. 185- 194, (2004).

[5] M. Buragohainand, and R. Velmurugan, "Optimal design of filament wound grid-stiffened composite cylindrical structures", *Defence Science Journal*, Vol. 61, No. 1, pp. 88-94, (2011).

[6] E. Wodesenbe, S. Kidane, and S.S. Pang, "Optimization for buckling loads of grid stiffened composite panels", *Composite Structures*, Vol. 60, No. 2, pp. 159-169, (2003).

[7] R. F. Gibson, "Energy Absorption in Composite Grid Structures", *Advanced Composite Materials*, Vol. 14, No. 2, pp. 113-119, (2005).

[8] R. Zamani, G. H Rahimi, M. H. Pol, and M. Hedayatian, "Reinforcing effect of nanoclay on buckling behavior of nanocomposite grid shells: Experimental investigation", *Modares Mechanical Engineering*, Vol. 15, No. 3, pp. 411-418, (2015).

[9] K. S. Pandya, and N. K. Naik, "Analytical and experimental studies on ballistic impact behavior of carbon nanotube dispersed resin", *International Journal of Impact Engineering*, Vol. 76, pp. 49-59, (2015).

[10] A. R. Sabet, M. H. Beheshty, and H. Rahimi, "High velocity impact behavior of GRP panels containing coarse-sized sand filler", *Polymer Composites*, Vol. 29, No. 8, pp. 932-938, (2008).

[11] U. Alkan, Y. Ozcanlı, and V. Alekberov, "Effect of temperature and time on mechanical and electrical properties of HDPE/glass fiber composites", *Fibers and Polymers*, Vol. 14, No. 1, pp. 115-120, (2013).

[12] A. Brenes-Acosta, and B. A. Stradi-Granados, "Comparative study of the mechanical properties of polyester resin with and without reinforcement with fiber-glass and furcraea cabuya fibers", *Fibers and Polymers*, Vol. 15, No. 10, pp. 2186-2192, (2014).

[13] J. Li, and Y. C. Xia, "The reinforcement effect of carbon fiber on the friction and wear properties of carbon fiber reinforced PA6 composites", *Fibers and Polymers*, Vol. 10, No. 4, pp. 519-525, (2009).

[14] R. Eslami-Farsani, H. Khosravi, and S. Fayazzadeh, "Using 3-Glycidoxy propyltrimethoxy silane functionalized SiO_2 nanoparticles to improve flexural properties of glass fibers/epoxy grid- stiffened composite panels", *International Scholarly and Scientific Research & Innovation*, Vol. 9, No. 12, pp. 1350-1353, (2015).

[15] A. Abdi, R. Eslami-Farsani, and H. Khosravi, "Evaluating the mechanical behavior of basalt fibers/epoxy composites containing surface-modified $CaCO_3$ nanoparticles", *Fibers and Polymers*, Vol. 19, No. 3, pp. 635-640, (2018).

[16] M. M. Shokrieh, A. Saeedi, and M. Chitsazzadeh, "Evaluating the effects of multi-walled carbon nanotubes on the mechanical properties of chopped strand mat/polyester composites", *Materials and Design*, Vol. 56, pp. 274-279, (2014).

[17] M. T. Byrne, and Y. K. Gunko, "Recent advances in research on carbon nanotube-polymer composites", *Advanced Materials*, Vol. 22, No. 15, pp. 1672-1688, (2010).

[18] Z. Spitalsky, D. Tasis, K. Papagelis, and C. Galiotis, "Carbon nanotube-polymer composites: chemistry, processing, mechanical and electrical properties", *Progress in Polymer Science*, Vol. 35, No. 3, pp. 357-401, (2010).

[19] H. Ulus, Ö. S. Şahin, and A. Avcı, "Enhancement of flexural and shear properties of carbon fiber/epoxy hybrid nanocomposites by boron nitride nanoparticles and carbon nanotube modification", *Fibers and Polymers*, Vol. 16, No. 12, pp. 2627-2635, (2015),

[20] K. S. Pandya, K. Akella, M. Joshi, and N. K. Naik, "Ballistic impact behavior of carbon nanotube and nanosilica dispersed resin and

composites", *Journal of Applied Physics*, Vol. 112, pp. 1-6, (2012).

[21] M. Rahman, M. Hosur, Sh. Zainuddin, U. Vaidya, A. Tauhid, A. Kumar, J. Trovillion, and Sh. Jeelani, "Effects of amino-functionalized MWCNTs on ballistic impact performance of E-glass/epoxy composites using a spherical projectile", *International Journal of Impact Engineering*, Vol. 57, pp. 108-118, (2013).

[22] S. Laurenzi R. Pastore G. Giannini, and M. Marchetti, "Experimental study of impact resistance in multi-walled carbon nanotube reinforced epoxy composite structures", *Composite Structures*, Vol. 99, pp. 62-68, (2013).

[23] M. M. Rahman, Sh. Zainuddin, and M. V. Hosur, "Improvements in mechanical and thermo-mechanical properties of e-glass/epoxy composites using amino functionalized MWCNTs", *Composite Structures*, Vol. 94, pp. 2397-2406, (2012).

[24] H. Khosravi, and R. Eslami-Farsani, "Reinforcing effect of surface-modified multiwalled carbon nanotubes on flexural response of E-glass/epoxy isogrid-stiffened composite panels", *Polymer composites*, Vol. 32, No. S2, pp. E677-E686, (2018).

[25] M. Hedayatian, G.H. Liaghat, Gh. Rahimi, M.H. Pol H. Hadavinia and R. Zamani, "Investigation of the high velocity impact behavior of grid cylindrical composite structures", *Polymer composites*, Vol. 38, No. 11, pp. 2603-2608, (2017).

[26] H. Khosravi, and R. Eslami-Farsani, "On the flexural properties of multiscale nanosilica/E-glass/epoxy anisogrid-stiffened composite panels", *Journal of Computational and Applied Research in Mechanical Engineering*, Vol. 7, No. 1, pp. 99-108, (2017).

[27] H. Khosravi, and R. Eslami-Farsani, "Enhanced mechanical properties of unidirectional basalt fiber/epoxy composites using silane-modified Na^+-montmorillonite nanoclay", *Polymer Testing*, Vol. 55, pp. 135-142, (2016).

[28] R. Eslami-Farsani, and A. Shahrabi-Farahani, "Improvement of high-velocity impact properties of anisogrid stiffened composites by multi-walled carbon nanotubes", *Fibers and Polymers*, Vol. 18, No. 5, pp. 965-970, (2017).

[29] Y. M. Jen, and C. Y. Huang, "Fatigue characterization of acid treated carbon nanotube/epoxy composites", *Journal of Composite Materials*, Vol. 47, No. 13, pp. 1665-1675, (2013).

[30] V. Brancato, A. M. Visco, and A. Pistone, "Effect of functional groups of multi-walled carbon nanotubes on the mechanical, thermal and electrical performance of epoxy resin based nanocomposites", *Journal of Composite Materials*, Vol. 47, No. 24, pp. 3091-3103, (2013).

[31] Y. B. Tee, R. A. Talib, and K. Abdan, "Thermally grafting aminosilane onto kenaf-derived cellulose and its influence on the thermal properties of poly (lactic acid) composites", *BioResources*, Vol. 8, No. 3, pp. 4468-4483, (2013).

[32] M. T. Kim, K. Y. Rhee, S. J. Park, and D. Hui, "Effects of silane-modified carbon nanotubes on flexural and fracture behaviors of carbon nanotube-modified epoxy/basalt composites", *Composites*, Vol. 43, No. 5, pp. 2298-2302, (2012).

[33] M. M. Rahman, S. Zainuddin, M. V. Hosur, C. J. Robertson, A. Kumar, J. Trovillion, and S. Jeelani, "Effect of NH_2-MWCNTs on crosslink density of epoxy matrix and ILSS properties of e-glass/epoxy composites", *Composite Structures*, Vol. 95, pp. 213-221, (2013).

[34] J. E. Garcia, B. L. Wardle, and A. J. Hart, "Joining prepreg composite interfaces with aligned carbon nanotubes", *Composites part A*, Vol. 39, No. 6, pp. 1065-1070, (2008).

[35] D. Micheli, A. Vricella, R. Pastore, A. Delfini, A. Giusti, M. Albano, M. Marchetti, F. Moglie, and M. V. Primiani, "Ballistic and electromagnetic shielding behavior of multifunctional Kevlar fiber reinforced epoxy composites modified by carbon nanotubes", *Carbon*, Vol. 104, pp. 141-156, (2016).

[36] J. Zhang, S. Jua, D. Jiang, and H. X. Peng, "Reducing dispersity of mechanical properties of carbon fiber/ epoxy composites by introducing multi-walled carbon nanotube", *Composites Part B*, Vol. 54, No. 1, pp. 371-376, (2013).

[37] S. Zhang, W. Liu, J. Wang, B. Li, L. Hao, and R. Wang, "Improvement of interfacial properties of carbon fiber-reinforced poly (phthalazinone ether ketone) composites by introducing carbon nanotube to the interphase", *Polymer Composites*, Vol. 36, No. 1, pp. 26-33, (2015).

[38] P. Udatha, C. V. S. Kumar, S. N. Nair, and N. K. Naik, "High velocity impact performance of three-dimensional woven composites", *The*

Journal of Strain Analysis for Engineering Design, Vol. 47, No. 7, pp. 419-431, (2012).

[39] H. Khosravi, and R. Eslami-Farsani, "On the mechanical characterizations of unidirectional basalt fiber/epoxy laminated composites with 3-glycidoxypropyltrimethoxysilane functionalized multi-walled carbon nanotubes-enhanced matrix", *Journal of Reinforced Plastics and Composites*, Vol. 35, No. 5, pp. 421-434, (2016).

How to cite this paper:

Hamed Khosravi and Reza Eslami-Farsani, "High-velocity impact properties of multi-walled carbon nanotubes/E-glass fiber/epoxy anisogrid composite panels", Journal of Computational and Applied Research in Mechanical Engineering, Vol. 9, No. 2, pp. 235-243, (2019).

DOI: 10.22061/jcarme.2018.3646.1425

URL: http://jcarme.sru.ac.ir/?_action=showPDF&article=922